

L-Serine Obtained by Methanol Addition in Batch Crystallization

Hervé Charmolue and Ronald W. Rousseau

School of Chemical Engineering, Georgia Institute of Technology, Atlanta, GA 30332

The solubility of L-serine in water was measured as a function of temperature, and the solubility in methanol-water solutions was determined as a function of temperature and methanol concentration. Solubility in aqueous solutions was found to be a linear function of temperature. Additionally, a statistical design of experiments was used to identify the kinetic variables that influence the purity of L-serine crystals recovered by batch crystallization. Agitation and the rate at which supersaturation was generated through cooling and methanol addition were found to influence the methanol content of the recovered crystals. The size of the recovered crystals also was found to depend on agitation and the rate at which methanol was added to the L-serine mother liquor.

Introduction

Although crystallization has been employed extensively as a separation process, purification techniques using crystallization have become more important in recent years. There is also an intense revival of commercial interest in batch processes, such as those found in the manufacture of high-value-added specialty chemicals, and the recovery and purification of such compounds frequently involve batch crystallization. An overriding concern in the production of specialty chemicals is product quality, which in the context of crystallization may mean purity, size, and morphology or habit. When these factors are taken together, the great concern over the reproducibility of crystal properties from one batch to the next becomes apparent.

It is important to understand the characteristics of crystals produced from batch crystallization to relate these characteristics to operational variables that control crystal properties. L-serine, $\text{HO-CH}_2\text{-CH(NH}_2\text{)-COOH}$, was chosen as a model system in the present research, and an experimental plan was developed, based on which general conclusions concerning crystal purity and batch crystallization protocol may be drawn. A second reason for choosing L-serine is that it has significance in the food and pharmaceutical industries. Industrial synthesis of this amino acid involves fermentation, and its recovery and purification utilize a combination of cooling and salting-out

by addition of methanol. Purity requirements are stringent, especially with regard to organic impurities such as methanol. Consequently, concerns about crystal purity are encountered in the process, and several redissolution-recrystallization steps may be required to meet specified standards.

Numerous mechanisms by which impurities can be incorporated into crystalline products have been studied including adsorption of impurities on crystal surfaces (Girolami and Rousseau, 1985), solvent entrapment in cracks, crevices and agglomerates, and inclusion of pockets of liquid (Hiquily and Laguérie, 1984). An impurity with a structure sufficiently similar to the material being crystallized can also be incorporated into the crystal lattice by substitution or entrapment (Balarew, 1982; Black and Davey, 1988). Among these mechanisms, inclusion formation has been extensively studied (Denbigh and White, 1966; Wilcox, 1968; Edie and Kirwan, 1973; Myerson and Kirwan, 1977a, b; Hiquily et al., 1985). It has also been suggested that the purity may be linked directly to size and habit of product crystals, but the interaction does not appear to be simple. Jenkins and Sinha (1984) have noted that the key to producing high-purity crystals was to maintain the supersaturation at a low level so that large crystals were obtained. In contrast, Hiquily et al. (1985) found that reducing the size of ammonium perchlorate crystals resulted in a substantial decrease of the moisture due to inclusion.

There were two major thrusts in the present work: measurement of the solubility of L-serine and determination of those factors that influence the purity of recovered crystals.

Correspondence concerning this article should be addressed to R. W. Rousseau.

Current address of H. Charmolue: Laboratoire Central du Service des Essences des Armées, 280, Chemin de Sainte Marthe, 13014 Marseille, France.

Solubility

Solubilities are the key to determining the recovery of materials achievable by crystallization, and they are required to quantify supersaturation, an important parameter in nucleation and growth kinetics. Solubility data for amino acids in aqueous solution are widely reported in the literature, but often such data appear to be inaccurate. The methods of isolation and detection, which were crude at the time the referenced measurements were taken, could explain this inaccuracy (Zumstein and Rousseau, 1989).

With the development of amino acid preparation by microbiological synthesis, however, it is now possible to produce such compounds at high purity. Also, progress in analytical chemistry, especially chromatographic techniques, provides accurate determination of amino acid purity. As a result, there is a need to review the data bank concerning amino acids solubilities. For example, the solubility of *L*-isoleucine in water has been measured recently (Zumstein, 1987; Gambrel, 1989) and found to differ significantly from those in the literature. The present work investigates the solubilities of *L*-serine in water and in water-methanol solutions.

Aqueous Solutions

Several experiments were conducted to estimate the time for solutions to come to equilibrium. This was accomplished by agitating a slurry of distilled water and an excess of *L*-serine crystals. The slurry was held for an hour at a temperature 10°C above that to be evaluated; it then was cooled to the desired temperature. After four hours, the agitation was stopped and the slurry was allowed to settle. A sample of the solution was recovered by filtering the liquid phase through an F11SVT ($\approx 0.4 \mu\text{m}$) Veriflo filter which was at the same temperature as the slurry. The density of the sample was measured using a precision densitometer and the *L*-serine concentration deduced from a calibration chart. The slurry was agitated once again, and four hours later the same procedure was repeated. The results in Table 1 show that after the initial four-hour period there was no change in concentration. Accordingly, the four-hour duration was taken as the time for solutions to reach equilibrium in subsequent experiments.

Solubilities were measured over the temperature range 3.5–50°C. A slurry of distilled water and excess *L*-serine crystals was heated to 60°C and cooled to 50°C. Four hours later, a sample was removed using the procedure described above, and its density was measured. The slurry was then cooled to the next desired temperature and allowed to equilibrate before another sample was removed (four hours later). A second set of experiments was performed by reversing the path so that instead of cooling to saturation, there was heating to saturation: that is, a slurry of excess *L*-serine crystals was

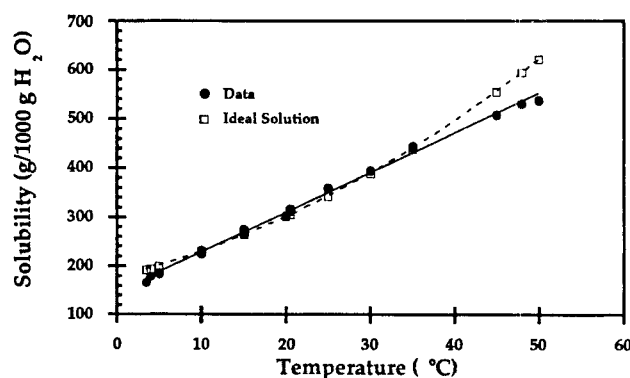


Figure 1. Solubilities of *L*-serine in water.

heated progressively starting from 3.5°C and going up to 50°C. At the beginning of the experiment, the same amounts of crystals and water as in the previous slurry were present in the vessel. The results are plotted in Figure 1. Regression of the data resulted in the equation

$$S = 146.1300 + 8.08347(T^{\circ}\text{C}) \quad (1)$$

which is plotted as the solid line through the data in Figure 1. The correlation coefficient of this fit was 0.996.

Figure 1 also shows comparisons between measured solubilities and predictions using ideal solution theory. This theory provides an estimate of the solubilities of solids in liquids when the chemical nature of the solute is similar to that of the solvent (Prausnitz et al., 1986),

$$\ln \frac{1}{x_2} = \frac{\Delta H_m^f}{RT_m} \left(\frac{T_m}{T} - 1 \right) \quad (2)$$

where x_2 is solute mole fraction at saturation, ΔH_m^f is the enthalpy of fusion at the melting point, and T_m the normal melting temperature in K.

Using Eq. 2 for serine requires knowledge of the normal melting temperature ($T_m = 501 \text{ K}$) and of the enthalpy of fusion at the melting point, which unfortunately is not available in the literature. However, Bondi (1967) presents a method of predicting the fusion entropy of crystals from their molecular structure and melting point. Using this procedure, the following relationship was determined:

$$\frac{\Delta S_m^f}{R} = \frac{\Delta H_m^f}{RT_m} = 4.25 \quad (3)$$

which gives the equilibrium mole fraction of *L*-serine in solution as:

$$x_2 = \exp \left[-4.25 \left(\frac{501}{T} - 1 \right) \right] \quad (4)$$

The solubility S in g/1,000 g of water is then given by:

$$S = M \frac{1000}{18} \frac{x_2}{1 - x_2} \quad (5)$$

where M is molecular weight of serine (105.1).

Table 1. Variation of *L*-Serine Concentration with Time at 20°C

Time h	Concentration g/1,000 g water
4.42	302.407 \pm 1.647
17.42	301.973 \pm 0.421
20.75	303.346 \pm 1.004
29.00	301.069 \pm 0.947

Agreement between predictions and measured values is indeed good, as shown in Figure 1. The approach, however, has not been tested with other amino acids.

Water-Methanol Solutions

The molecular interactions between the solvent and the polar groups of *L*-serine influence *L*-serine solubility; although such influences can be explained in terms of dependence of the *L*-serine activity coefficient on solvent, the inability to predict the dependence makes solubility estimates difficult, if not impossible. The difficulty resides in the complex behavior of amino acids in solution; they exhibit chemical properties similar to those of weak electrolytes (dissociation in acidic, basic or zwitterionic forms), combined with different types of interactions (ionic, polar, dipolar or nonpolar) with the surroundings. An attempt to derive a solid-liquid equilibrium expression suitable for amino acids has been made by Nass (1988), who separated the activity coefficient into two independent terms: one arising from chemical interactions and the other from physical interactions. The chemical term was modeled by chemical theory, while physical interactions were accounted for by a form of the Wilson equation. Another approach has been proposed by Gupta and Heidemann (1990). The use of the modified UNIFAC group contribution model (Larsen et al., 1987) is recommended to evaluate activity coefficients. Coon et al. (1988) reported excellent predictions of the Scatchard-Hildebrand theory for polynuclear aromatic hydrocarbons in both pure and mixed organic solvents. Orella and Kirwan (1989) review the methods that can be employed to correlate the activity coefficients.

Rather than depending on the uncertainty of predictions arising from the models described in the preceding paragraph, experimental measurements were obtained of the effect of methanol on *L*-serine solubility. A known volume of methanol was mixed with a known volume of water in a 20-mL vial. Accordingly, the volume used in the present work is determined from a knowledge of the volumes of pure water and pure methanol. An excess of *L*-serine crystals was added to the contents of the vial, which then was sealed with a stopper and placed in a water bath. The temperature of the bath was controlled to $\pm 0.05^\circ\text{C}$ of the setpoint and was measured with a

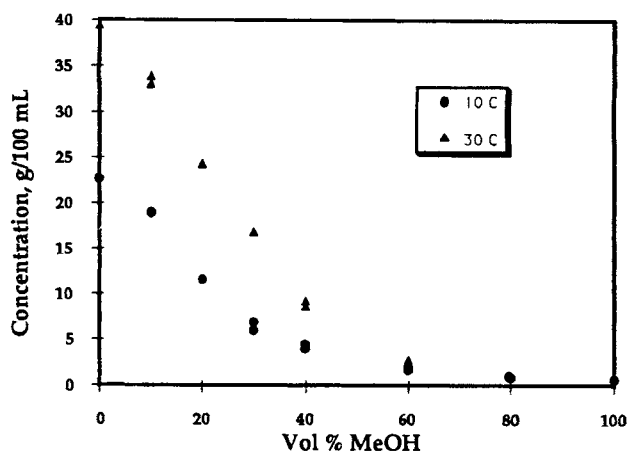


Figure 2. Solubility of *L*-serine in methanol-water solutions.

calibrated thermometer. The slurry was heated 10°C above the desired temperature for an hour, cooled to the desired temperature, and allowed to equilibrate. Twelve hours later, samples were removed and filtered through a $0.45\text{-}\mu\text{m}$ glass-fiber filter. The amount of *L*-serine in the filtrate was determined by HPLC analysis. The pH of the solution was at the isoelectric point ($\text{pH} = 5.68$). The solubility data of *L*-serine in water/methanol mixtures were obtained over the range 0 to 100 vol. % methanol at 10°C and 30°C (see Table 2 and Figure 2).

Relative solubility is defined by the ratio of the solubility in a mixed-solvent system to the solubility in water at the same temperature. Figure 3 shows the variation of the relative solubility of *L*-serine with the composition of the mixed solvent. The near linearity of the graphical representation and coincidence of data for different temperatures make Figure 3 useful in interpolation and extrapolation of the limited data.

The solubility of *L*-serine is temperature- and pH-dependent, and strongly influenced by the nature of the solvent. Orella and Kirwan (1989) have studied the effects of different aliphatic alcohols on the solubilities of several amino acids. They observed that the magnitude of the effect is smaller for amino acids with a nonpolar side chain than for those with a polar

Table 2. Solubility in Methanol-Water Solutions

Vol. % MeOH	<i>L</i> -serine Concentration, g/100 mL	
	10°C	30°C
0 ± 0.5	22.715 ± 1.161	39.404 ± 1.072
10 ± 0.5	18.902 ± 0.798	33.039 ± 0.541
10 ± 0.5	19.055 ± 1.078	33.897 ± 0.799
20 ± 0.5	11.576 ± 1.479	24.380 ± 1.004
20 ± 0.5	11.592 ± 1.030	24.276 ± 2.001
30 ± 0.5	5.951 ± 1.931	16.900 ± 1.284
30 ± 0.5	6.879 ± 1.020	16.874 ± 1.913
40 ± 0.5	3.957 ± 1.468	9.259 ± 0.132
40 ± 0.5	4.453 ± 1.419	8.643 ± 1.834
60 ± 0.5	1.637 ± 1.347	2.748 ± 1.007
60 ± 0.5	1.970 ± 1.008	2.493 ± 1.386
80 ± 0.5	0.838 ± 0.566	0.962 ± 0.439
80 ± 0.5	0.864 ± 0.731	0.969 ± 0.992
100 ± 0.5	0.592 ± 0.471	0.701 ± 0.756
100 ± 0.5	0.708 ± 0.697	0.705 ± 0.674

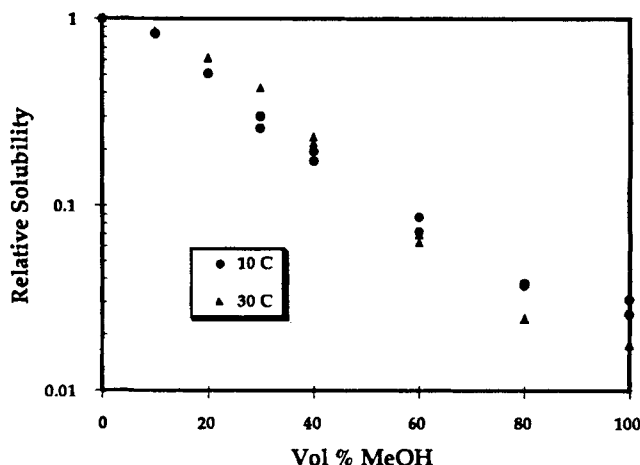


Figure 3. Relative solubilities of *L*-serine in MeOH-water solutions.

side chain. Therefore, alcohols would be better crystallizing agents, in terms of yield, for amino acids with polar side chains. The data obtained for serine illustrate that observation; relative solubility is reduced by two orders of magnitude with addition of methanol. The reduction factor seems to be the same at both 10 and 30°C.

Batch Crystallizations

Batch crystallizations were conducted in a 600-mL glass, jacketed vessel equipped with baffles to insure proper mixing and a cover to minimize evaporation and external contamination. Mechanical agitation was provided by a marine-type teflon impeller (7-mm-diameter). The temperature of the crystallizer was controlled by circulation of water from a constant-temperature bath and was measured with a calibrated thermometer. *L*-serine was obtained from an industrial source and was found to have an assay of 97% and 3% of other amino acids. It was used without further purification.

Experiments began by charging the crystallizer with 22.5 g of *L*-serine and 50 mL of distilled water. The resulting mixture was heated to 50°C so that all crystals were dissolved and the solution was perfectly clear. The temperature was then brought to 40°C. The agitator speed was set at a particular value, and the temperature of the crystallizer was lowered at a selected rate to 10°C. Seventy-five mL of methanol was added to the mixture at a fixed rate when the temperature reached 10°C. The crystallizer temperature was maintained at $10 \pm 0.05^\circ\text{C}$ for an hour. The agitation was then stopped, and crystals were removed by filtration through a $1.5\text{-}\mu\text{m}$ glass-fiber filter. The recovered crystals were allowed to dry for 24 hours at atmospheric pressure in an oven whose temperature was controlled to $75 \pm 0.5^\circ\text{C}$.

Analytical Methods

The crystal purity was determined the day after crystallization using the following procedure. Approximately 0.75 g of recovered *L*-serine crystals was redissolved in 25 mL of distilled water. High-performance liquid chromatography (HPLC) was used to measure the *L*-serine content of the sample, while the methanol content was determined by gas chromatography (GC). The values determined from GC and HPLC analyses were used to determine the purity of the recovered crystals in terms of parts per million (ppm) methanol. Details are given by Charmolue (1990).

Effects of Process Variables on Crystal Purity

A factorial design of experiments, as suggested by Box et al. (1978), was established to identify the key variables influencing the methanol content of *L*-serine crystals. With this type of design, the influence of each process variable at a variety of levels of the other variables can be observed, greatly facilitating the discovery of similarities and simplifications and estimations of interactions among the variables. The experimental plan was to focus on those variables that were thought to have the greatest influence on nucleation and growth kinetics; therefore, the variables chosen for examination were agitation as reflected by the agitator speed and the rates at which supersaturation were generated through cooling and

Table 3. 2^3 Factorial Design

Process Variable	Level	
	–	+
X_1 , Agitation Speed, rpm	500	1,500
X_2 , Cooling Rate, $^\circ\text{C}/\text{h}$	10	48
X_3 , Methanol Addition Rate, mL/min	6	24

Table 4. Results of the 2^3 Factorial Design

Run	X_1	X_2	X_3	R , ppm	L , μm	L/W
1	–	–	–	746 ± 85	990 ± 55	1.44 ± 0.10
2	+	–	–	498 ± 98	326 ± 87	1.39 ± 0.10
3	–	+	–	$1,326 \pm 74$	728 ± 61	1.92 ± 0.09
4	+	+	–	992 ± 93	395 ± 96	1.24 ± 0.22
5	–	–	+	603 ± 108	520 ± 68	1.73 ± 0.06
6	+	–	+	420 ± 75	290 ± 52	1.41 ± 0.03
7	–	+	+	$1,430 \pm 89$	563 ± 56	1.31 ± 0.05
8	+	+	+	$1,020 \pm 95$	382 ± 69	1.27 ± 0.28

Table 5. Calculated Effects and Standard Errors for the 2^3 Factorial Design

Effect	Purity Estimate \pm Standard Error
<i>Average</i>	879.37 ± 31.80
<i>Main Effects</i>	
X_1 , Agitation	-293.00 ± 63.60
X_2 , Cooling Rate	625.25 ± 63.60
X_3 , MeOH Addition Rate	$-1,036.00 \pm 63.60$
<i>Two-Factor Interactions</i>	
X_1X_2	-78.25 ± 63.60
X_1X_3	-2.75 ± 63.60
X_2X_3	88.25 ± 63.60
<i>Three-Factor Interaction</i>	
$X_1X_2X_3$	-35.25 ± 63.60

addition of methanol. This meant that our case corresponded to a 2^3 factorial design (three variables at two levels). Table 3 gives the chosen levels for each variable. The experimental design required eight runs to study all the possible variable combinations. Results of these experiments are given in Table 4. The level of each variable during a run is indicated in columns 2 to 4, and the residual amount of methanol R found in the crystals for each set of conditions is shown in column 5. Each of these values is an average of two sets of experiments that were run in slightly different crystallizers, which were operated simultaneously to insure that the controlled variables in each were the same. The difference between the two crystallizers was in the baffles used to aid mixing: in one they were attached to the cover plate, while in the other they were attached to the crystallizer wall.

Estimates of the effects of the experimental variables were calculated following the procedure recommended by Box et al. (1978) (see Table 5). The standard errors were obtained using data from the pair of crystallizers operated as described. Comparison of the estimates with their standard errors suggests the following conclusions. The main effects of the agitation rate X_1 , the cooling rate X_2 , and the methanol addition rate, X_3 require further interpretation, while there is no evidence of any two-variable or three-variable interactions. The main ef-

fects, therefore, can be interpreted individually: the effect of a single variable at selected fixed conditions of the others could be investigated and it would be relevant to draw conclusions from the results.

Agitation

The effect of agitation on crystal purity was examined through batch crystallizations performed as described previously. The cooling and methanol addition rates were fixed at 48°C/h and 6 mL/min, respectively, while the agitator speed was varied from 500 rpm to 1,500 rpm. As shown in Figure 4, the purity of the recovered crystals increased with agitation until an impeller speed of about 1,000 rpm was reached; thereafter, the purity of the crystals was diminished with increased agitation.

The results shown in Figure 4 were explained through further observations of the crystal samples obtained from these experiments. When the agitation inside the crystallizer was relatively low, large agglomerated crystals ($> 1,000 \mu\text{m}$) were obtained. Solvent could easily be trapped between the individual crystals forming the agglomerates. As the agitation was increased, the number of monocrystals forming an agglomerate decreased; as a result, the residual amount of methanol found in the recovered crystals was reduced and the purity increased. The highest purity (650 ppm) was obtained when there were no agglomerates, that is, when the crystals were monocrystals. Even for monocrystals, traces of methanol were still detected. This would suggest that entrapment of methanol between agglomerates is not the only mechanism of methanol incorporation. Methanol could be included in the crystal or adsorbed on the crystal surface. The drastic change in the purity occurring under high stirring conditions is believed to be the result of crystal breakage; the external shape of crystals produced in this operating regime was not well defined and agglomerates reformed.

Cooling rate

The cooling rate was varied in the range 10°C/h to 48°C/h, while agitation and methanol addition rates were maintained at 1,500 rpm and 24 mL/min, respectively. As shown in Figure 5, crystal purity exhibited a strong dependence on the rate at which supersaturation was generated. The amount of methanol found in the crystals was reduced by half when the cooling rate was changed from 48°C/h to 10°C/h. The dependence appears to be linear in the range explored.

In addition to noting the changes in purity reflected in Figure 5, the temperature at which nucleation occurred also changed with the cooling rate. Nucleation occurred at 25°C when the cooling rate was 48°C/h, whereas nuclei appeared at 20°C when the cooling rate was fixed at 10°C/h. This difference in the temperature of nucleation has a significant influence on the supersaturation at nucleation; specifically, as the temperature of nucleation is decreased, the supersaturation is increased. Such a situation should mean that the number of *L*-serine crystals produced during the cooling portion of the protocol should be larger when the cooling rate is lower. Accordingly, subsequent addition of methanol would occur with greater available surface area for growth. These factors could represent the reason for the increase in purity (decrease in methanol content) as cooling rate is decreased.

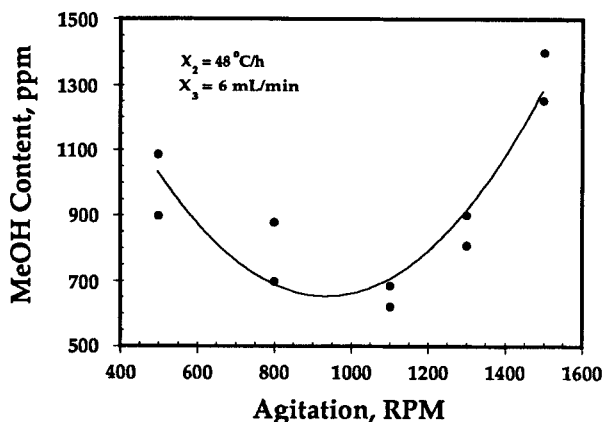


Figure 4. Effect of agitation on the purity of *L*-serine crystals.

Methanol addition rate

Several crystallizations were performed in which methanol was added at different rates; in these experiments, agitation was set at 1,500 rpm and the cooling rate at 48°C/h. The purity of the crystals obtained was analyzed as shown in Figure 6. It is noted that the results differed significantly among replicated runs, but the trends were the same; there was a slight decrease in purity with an increase in the methanol addition rate. It is suspected that the relatively minor impact of the methanol addition rate is due to a heat effect associated with adding methanol at a temperature greater than the temperature of the crystallizing medium. Recall that methanol addition began when the temperature of the crystallizing medium was at 10°C. In this series of experiments, the temperature increased to 13°C when methanol was added at a rate of 6 mL/min, but it went to 20°C when the addition rate was 24 mL/min. The temperature increase was calculated to be only 3°C when based only on the heat of methanol solution and the sensible heat provided by the added methanol. Therefore, the observed increase in temperature certainly is associated with nucleation.

The thermal effects, described in the preceding paragraph, along with the usual competition between nucleation and growth for available supersaturation, are thought to have diminished the expected effect of methanol addition rate. In a

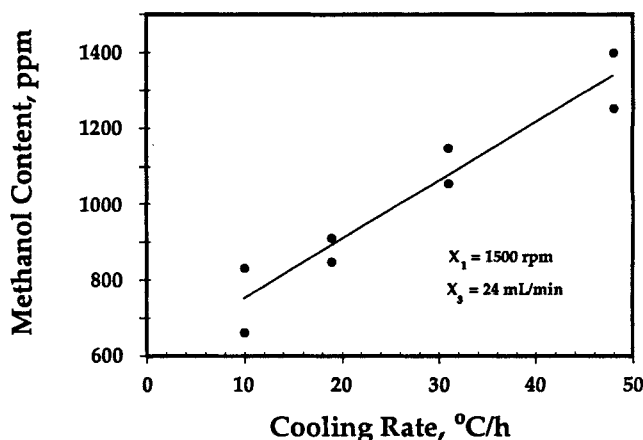


Figure 5. Effect of cooling rate on the purity of *L*-serine crystals.

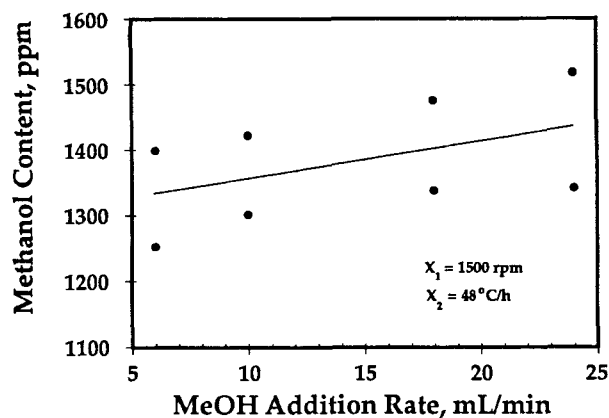


Figure 6. Effect of methanol addition rate on the purity of *L*-serine crystals.

competitive process, a high methanol addition rate causes a sudden high level of supersaturation that favors nucleation over crystal growth and produces large numbers of small crystals. However, the large surface area generated means that crystal growth can proceed without some of the usual inclusions associated with growth onto limited surface area and high supersaturation. It was observed that the purity of crystals recovered from a batch crystallization correlated with a measure of crystal size. This observation is discussed completely in a later section. An additional observation regarding the lower-than-expected impact of increasing the methanol addition rate is that the smaller crystals formed with an increase in addition rate exhibited a lower degree of agglomeration.

Size and Habit of *L*-Serine Crystals

Since the purity of recovered *L*-serine crystals seemed to be influenced by the size and shape of the crystals, the effects of operational variables on crystal habit and size were investigated. As before, a factorial design was established to identify key variables affecting size and habit of *L*-serine crystals. Samples of crystals obtained from crystallizations at selected conditions were sized under a microscope by counting all those that were unbroken and within a fixed area on the microscope plate; the number of crystals sized was always greater than thirty, and the mean crystal size was the arithmetic average of the sizes determined. Figure 7 shows how size and habit were defined; *L* was the largest dimension of the crystal and *W* the smallest. The size was characterized by *L* and the habit by the ratio *L/W*. Based on a statistical analysis of the measurements, mean values for *L* and *L/W* were determined, as listed in Table 4. As before, calculated effects and standard errors were determined and compared.

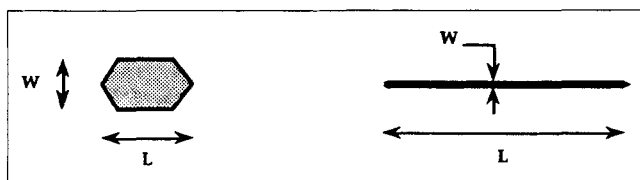


Figure 7. Characterization of crystal size and habit.

Table 6. Calculated Effects on Crystal Size and Standard Errors for the 2^3 Factorial Design

Effect	Size Estimate ± Standard Error
Average	524.25 ± 24.54
Main Effects	
X_1 , Agitation	-352.00 ± 49.08
X_2 , Cooling Rate	-14.5 ± 49.08
X_3 , MeOH Addition Rate	-171.00 ± 49.08
Two-Factor Interactions	
X_1X_2	95.00 ± 49.08
X_1X_3	146.5 ± 49.08
X_2X_3	82.00 ± 49.08
Three-Factor Interaction	
$X_1X_2X_3$	-70.50 ± 49.08

Crystal size

Estimates of the effects of the factorially designed experiments are given in Table 6. Agitation and methanol addition rates were found to be the key variables determining the size of *L*-serine crystals. The effect of the cooling rate was not statistically significant, and the factorial design also revealed the existence of an interaction between the agitation rate and the methanol addition rate: the effect of agitation depends on the level of the methanol addition rate and *vice versa*. Thus, these two variables were considered jointly in the study of the effects of operating variables on crystal size, and a series of experiments gave the results shown in Figure 8.

The response surface in Figure 9 is an alternative convenient representation of the relationship found between size and agitation and methanol addition rate. Note that an increase in agitation and methanol addition rate resulted in a reduction in crystal size. As an illustration, the size of *L*-serine crystals was reduced by 67% when the agitation rate was increased by a factor of 3 with the methanol addition rate maintained at a constant value of 6 mL/min. At low and constant agitation (500 rpm), a change from 6 mL/min to 24 mL/min in the methanol addition rate diminished the crystal size by 47%. As the agitation is increased, the effect of the rate at which methanol was added was less important. Under high agitation (1,500 rpm), there was no effect of the rate at which methanol was added, and the crystal size was dictated only by the stirring

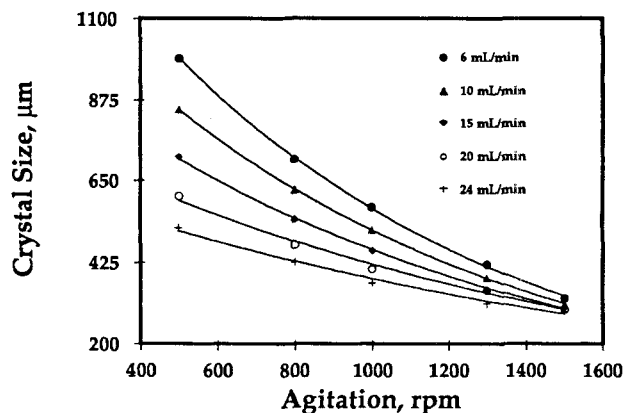


Figure 8. Effect of methanol addition rate and agitation on crystal size.

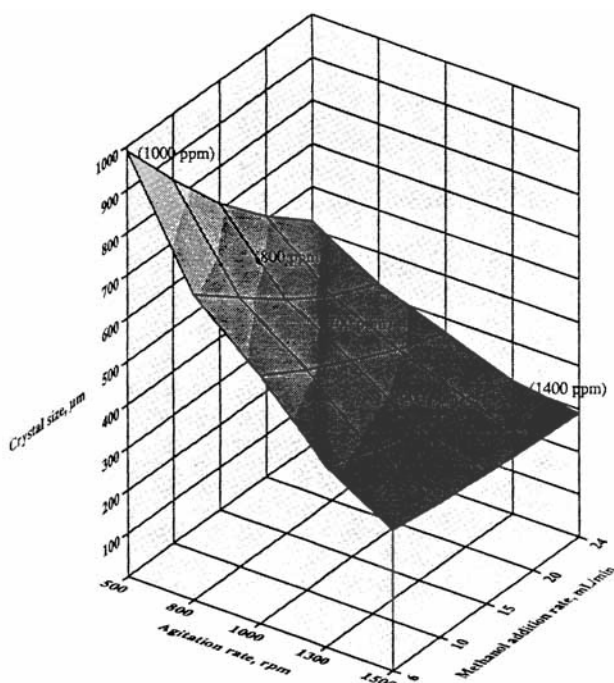


Figure 9. Response surface: effect of agitation and methanol addition rate on size and purity of *L*-serine crystals.

conditions. Similarly, agitation had less effect on crystal size as the methanol addition rate became more rapid.

A secondary observation resulting from these experiments is that the final product purity correlated with the ultimate size of the product crystals. This is shown by the different shaded areas on the response surface in Figure 9. The highest purity (≈ 700 ppm) was associated with crystal sizes ranging from 400 to 500 μm .

Crystal habit

Estimates of the effects of the factorially designed experiments are given in Table 7. None of the investigated variables were found to have a significant effect on crystal habit. Over the range of variables examined in this portion of the work, all crystals were obtained in the form of hexagonal blades (Figure 7). This habit was not altered by changing the levels of operational variables.

Despite the observations cited in the preceding paragraph, a series of experiments were performed in which a variable amount of methanol was added to a constant volume of *L*-serine solution. Specifically, saturated solutions of *L*-serine in water at 30°C (50 g of *L*-serine in 100 mL of water) and at 10°C (28.8 g of *L*-serine in 100 mL of water) were subjected to additions of methanol. The methanol volumes were 30, 50 and 100 mL, and the temperature of the methanol was the same as that of the *L*-serine solution to which it was added. The methanol was added rapidly, and one hour after addition, crystals were filtered and observed under an optical microscope. All crystals retained the hexagonal shape shown in Figure 7, except for those obtained as a result of adding an equal volume of methanol to the *L*-serine solutions. For this set of conditions, the ratio of the largest to the smallest crystal di-

Table 7. Calculated Effects on Habit and Standard Errors for the 2^3 Factorial Design

Effect	Habit (L/W) Estimate \pm Standard Error
<i>Average</i>	1.46 ± 0.05
<i>Main Effects</i>	
X_1 , Agitation	-0.27 ± 0.10
X_2 , Cooling Rate	-0.06 ± 0.10
X_3 , MeOH Addition Rate	-0.07 ± 0.10
<i>Two-Factor Interactions</i>	
X_1X_2	-0.09 ± 0.10
X_1X_3	0.09 ± 0.10
X_2X_3	-0.22 ± 0.10
<i>Three-Factor Interaction</i>	
$X_1X_2X_3$	0.23 ± 0.10

mension (L/W) was modified from about 1.5 to roughly 16. It is believed that structural factors of the crystal and associated bonds along with external factors such as crystallization conditions and solvent composition contribute to the habit modification. X-ray analysis has indicated subsequently that crystals recovered at high concentrations of methanol in the solution are of an anhydrous form as opposed to the monohydrate species recovered in other experiments.

The residual amount of methanol present in crystals having different habit, but formed under similar conditions, was also measured to determine whether a hexagonal shape or a needle-like habit was preferable in terms of purity. The purity was three times higher for hexagonal crystals than for needles.

Conclusions

An experimental program following a factorial design revealed that each of the investigated process variables (agitation, cooling rate, and methanol addition rate) individually influenced the purity of *L*-serine crystals. An agitator speed of 1,100 rpm was found to produce crystals of the greatest purity; examination of the crystals showed that under this stirring condition, no agglomerates were formed, no crystal breakage occurred, and only monocrystals were obtained. The size of the crystals recovered from the batch experiments depended on agitation and methanol addition rates only; a joint effect of these two variables was also observed. The effects of process variables on crystal habit were not statistically significant in the range of variables covered by the factorial design.

Purity, size, and habit appeared to be closely related. Crystals of the highest purity were produced when the crystal size was between 400 and 500 μm . The purity was also influenced strongly by the crystal morphology. A high level of supersaturation, brought about by the addition of a large quantity of methanol, was found to alter the crystal habit from hexagonal to needle-like. This habit modification was accompanied by a drastic decrease of the purity.

To minimize the methanol content of the crystals, agitation should be set to avoid agglomerate formation or crystal breakage. Supersaturation should be kept at a low level and carefully controlled when methanol is added as a precipitant to prevent the formation of needles.

Acknowledgment

The National Science Foundation (Grant No. CBT-8722281) is grate-

fully acknowledged for providing support for this research. Appreciation is expressed for the L-serine provided by Ajinomoto USA, Inc.

Literature Cited

- Armstrong, F. B., *Biochemistry*, 2nd ed., Oxford University Press, New York (1983).
- Balarew, C., "Inclusion of Isomorphous Admixtures in Crystal Hydrate Salts," *Industrial Crystallization*, S. J. Jancic and E. J. de Jong, eds., North-Holland Publishing Co., Amsterdam (1982).
- Black, S. N., and R. J. Davey, "Crystallization of Amino Acids," *J. Cryst. Growth*, **90**, 136 (1988).
- Bondi, A., "A Correlation of the Entropy of Fusion of Molecular Crystals with Molecular Structure," *Chem. Rev.*, **67**, 565 (1967).
- Box, G. E. P., W. G. Hunter, and J. S. Hunter, *Statistics for Experimenters*, p. 306, Wiley-Interscience (1978).
- Charmolue, H., "The Effects of Process Variables on Purity, Size and Habit of L-Serine Crystals Recovered by Batch Crystallization," MS Thesis, Georgia Institute of Technology, Atlanta (1990).
- Coon, J. E., W. B. Sediawan, J. E. Auwaerer, and E. McLaughlin, "Solubilities of Families of Heterocyclic Polynuclear Aromatics in Organic Solvents and Their Mixtures," *J. Sol. Chem.*, **17**, 519 (1988).
- Dalton, J. B., and C. L. A. Schmidt, "The Solubilities of Certain Amino Acids in Water, the Densities of Their Solutions at Twenty-Five Degrees," *J. Bio. Chem.*, **109**, 241 (1935).
- Denbigh, K. G., and E. T. White, "Studies on Liquid Inclusions in Crystals," *Chem. Eng. Sci.*, **21**, 739 (1966).
- Dunn, M. S., F. J. Ross, and L. S. Read, *J. Bio Chem.*, **103**, 579 (1933).
- Edie, D. D., and D. J. Kirwan, "Impurity Trapping during Crystallization from Melts," *Ind. Eng. Chem. Fundam.*, **12**, 100 (1973).
- Gambrel, T. W., "Batch Crystallization and Crystal Purity," MS Thesis, Georgia Institute of Technology, Atlanta (1989).
- Girolami, M. W., and R. W. Rousseau, "The Effects of Bismark Brown R on the Growth Rates of Large and Small Potassium Alum Crystals," *J. Cryst. Growth*, **71**, 220 (1985).
- Gupta, R. B., and R. A. Heidemann, "Solubility Models for Amino Acids and Antibiotics," *AIChE J.*, **36**, 333 (1990).
- Hiquily, N., and C. Laguérie, "Inclusion Formation in the Ammonium Perchlorate Crystals—Influence of Surfactants," *Industrial Crystallization*, p. 79, S. J. Jancic and E. J. de Jong, eds., Elsevier, Amsterdam (1984).
- Hiquily, N., C. Laguérie, and J. P. Couderc, "Analyse Expérimentale de la Formation d'Inclusions au Cours de la Cristallisation du Perchlorate d'Ammonium en Solution Aqueuse," *Chem. Eng. J.*, **30**, 1 (1985).
- Jenkins, D. H., and H. N. Sinha, "Crystallization of High-Purity Aluminum Chloride Hexahydrate for the Production of Alumina," *Industrial Crystallization*, p. 159, S. J. Jancic and E. J. de Jong, eds., Elsevier, Amsterdam (1984).
- Larsen, B. L., P. Rasmussen, and A. Fredenslund, "A Modified UNIFAC Group-Contribution Model for Prediction of Phase Equilibria and Heats of Mixing," *Ind. Eng. Chem. Res.*, **26**, 2274 (1982).
- Millipore Waters Associates, Bulletin B80 82564 (1984).
- Myerson, A. S., and D. J. Kirwan, "Impurity Trapping during Dendritic Crystal Growth: 1. Computer Simulation," *Ind. Eng. Chem. Fundam.*, **4**, 414 (1977a).
- Myerson, A. S., and D. J. Kirwan, "Impurity Trapping during Dendritic Crystal Growth: 2. Experimental Results and Correlation," *Ind. Eng. Chem. Fundam.*, **4**, 420 (1977b).
- Nass, K. K., "Representation of the Solubility Behavior of Amino Acids in Water," *AIChE J.*, **34**, 1257 (1988).
- Needham, T. E., A. N. Paruta, and R. J. Gerraughty, *J. Pharm. Sci.*, **60**, 565 (1971).
- Orella, C. J., and D. J. Kirwan, "The Solubility of Amino Acids in Mixtures of Water and Aliphatic Alcohols," *Bio. Prog.*, **5**, 89 (1989).
- Prausnitz, J. M., R. N. Lichtenthaler, and E. G. de Azevedo, *Molecular Thermodynamics of Fluid-Phase Equilibria*, 2nd ed., Prentice-Hall, Englewood Cliffs, NJ (1986).
- Wilcox, W. R., "Removing Inclusions from Crystals by Gradient Techniques," *Ind. Eng. Chem.*, **60**, 13 (1968).
- Zumstein, R. C., "1. Modeling, Determination, and Measurement of Growth Rate Dispersion in Crystallization; 2. The Crystallization of L-Isoleucine in Aqueous Solutions," PhD Thesis, North Carolina State Univ., Raleigh (1987).
- Zumstein, R. C., and R. W. Rousseau, "Solubility of L-Isoleucine in and Recovery of L-Isoleucine from Neutral and Acidic Aqueous Solutions," *Ind. Eng. Chem. Res.*, **28**, 1226 (1989).

Manuscript received Feb. 20, 1991, and revision received July 9, 1991.